Presegmentation-based adaptive CFAR detection for HFSWR

Jan Oliver Hinz*, Martin Holters*, Udo Zölzer*, Anshu Gupta† and Thomas Fickenscher†
*Department of Signal Processing and Communications
Helmut Schmidt University, Holstenhofweg 85, 22043 Hamburg, Germany
email: jan.hinz@hsu-hh.de
†Department of High-Frequency Engineering
Helmut Schmidt University, Holstenhofweg 85, 22043 Hamburg, Germany

***Abstract*— Common tasks of High-Frequency Surface Wave Radars (HFSWRs) are long-range ocean state monitoring and maritime surveillance with a strong focus on the detection of ships. Due to the heterogeneous background composed of sea-clutter and external noise the application of Constant False Alarm Rate (CFAR) algorithms with a single parameter set are likely to lead to a high probability of false alarm or poor detection performance.**

This paper is about adaptive CFAR with presegmentation, where the presegmentation is performed globally on each range-Doppler map and divides the detection background into external noise dominated regions and sea-clutter dominated regions. With this global knowledge it is possible to individually adapt the shape of the reference window for each Cell Under Test (CUT) to obtain homogeneous reference cells and avoid clutter-edges in the reference window. To further increase detection performance, the constant scale factor is chosen with respect to the current background. This enables detection of small targets in clutter while maintaining a low false-alarm rate for targets in external noise. To prevent the saturation of the tracker, a pretracker structure is presented which distinguishes between strong and weak detections and assigns priority to strong detections.

I. Introduction

High-Frequency Surface Wave Radars (HFSWRs) can be used for ocean state monitoring or ship detection. Due to the comparatively low operating frequencies these radars experience low attenuation and offer long-range surveillance capabilities. Hereby the detection of ships is either sea-clutter- or external noise limited. Especially difficult is the detection of ships at the borders between both detection backgrounds, commonly denoted as clutter edges.

In the past, 2- or 3-dimensional Constant False Alarm Rate (CFAR) target detection algorithms [1] have been used. Still in most cases only a single set of parameters (number of reference/guard cells, constant scale factor, reference window shape, etc.) has been used. As the typical CFAR algorithms are designed for a homogeneous detection background and the typical HFSWR background is likely to be inhomogeneous, applying a single detection parameter set to the Azimuth-Range-Doppler (ARD) data is either likely to result in an unacceptable high probability of false alarm or missed detections. This either results in a saturation of the tracker or an underperforming radar system.

To overcome these problems we propose the following detection approach, which can be best described as a two-step process. First a global segmentation strategy of the ARD into different background areas is performed. The segmentation is based on power values and a-priori knowledge of the first-order sea-clutter characteristics according to the model in [2]. Global here refers to the fact that we perform the segmentation on a global scale and not like many other CFAR approaches based on a local predefined reference window, as in composite-, ordered-statistic (OS-), adaptive-ordered statistic (AOS-) or variability-index (VI-) CFAR [3][4][5][6]. Second, an adaptive CFAR detector based on the segmentation result is applied. It adapts the shape of the reference cell window to obtain a homogeneous detection background and thus avoids clutter-edges in the reference cells. In addition the constant scale factor, as a function of the current background, is adapted.

The paper starts with a short summary of the detection background of HFSWRs in Section II, followed by a description of the proposed segmentation in Section III. Then, in Section IV a review of existing CFAR approaches, the proposed adaptive CFAR approach and the pretracker structure are described. In Section V the results of the evaluation are presented, followed by a conclusion in Section VI.

II. Detection Background

The detection background is composed of external noise and sea-clutter dominated areas and their respective transition areas. External noise is composed of galactic- and cosmic-noise as well as interference from radio-stations and lightning strikes. Generally external noise dominates most parts of the ARD data, where in this case it is assumed to be spectrally white in each dimension.

Sea-clutter in the HF domain mainly consists of two components: a dominant first-order component (the two so-called Bragg lines) and a less dominant second-order component [7]. Sea-clutter is due to the interaction of the vertically polarized electromagnetic wave with the approaching/receding gravity sea waves [2]. In case of the first-order sea-clutter, this occurs at a resonance wavelength following the relationship $\lambda_{\mathrm{water}} \approx \frac{1}{2}\lambda_{\mathrm{elec}}$. Due to the movement of the approaching/receding gravity sea waves they reflect energy with an approximate

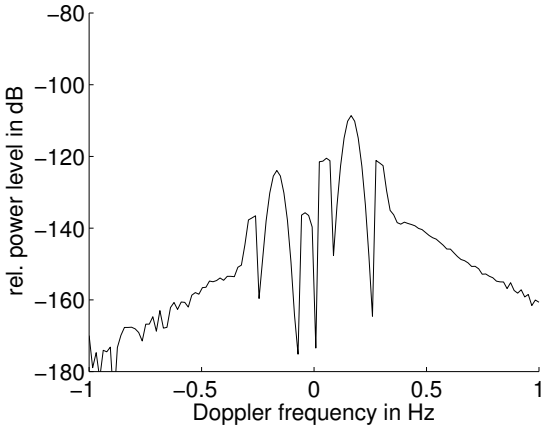

Fig. 1. Sea-clutter Doppler profile

Doppler-shift of

$$f_d = \pm\sqrt{\frac{g \cdot f}{\pi \cdot c}}, \tag{1}$$

where g is used to denote the standard gravity, f denotes the operating frequency of the radar and c is used to denote the speed of light [8]. The less-dominant second-order sea-clutter is due to multiple scattering of the electromagnetic wave by the gravity sea waves.

A typical Doppler profile with first- and second-order sea-clutter is illustrated in Fig. 1, with the first-order sea-clutter situated at a Doppler frequency of $\pm\,0.2\,\mathrm{Hz}$. In case an additional underlying radial sea current is present an additional Doppler shift occurs.

III. Background Segmentation

Our proposed detection approach starts with the presegmentation, which works on beamformed and range-Doppler processed (ARD) data. The first step is to distinguish between first-order sea-clutter dominated regions and external noise dominated regions, which involves the following tasks to be solved:

- calculation of the theoretical first-order sea-clutter Doppler frequency
- estimation of the true first-order sea-clutter Doppler frequency
- estimation of the first-order sea-clutter extent in Doppler domain
- external noise estimation
- estimation of the first-order sea-clutter extent in range domain

A. Theoretical and estimated first-order sea clutter Doppler frequency

First, the sum of the power values from all range bins for each particular Doppler bin k is calculated

$$p_k = \sum_{n=1}^{N} P_{k,n}, \qquad k = 1, \ldots, K \tag{2}$$

where $P_{k,n}$ is the power at the kth Doppler- and the nth range-cell. N and K are used to denote the total number of range- and Doppler-cells, respectively. Under the assumptions of random target distributions in terms of range and Doppler, the summation (2) emphasizes the regions of sea-clutter and reduces the impact of targets at particular range-Doppler combinations.

Secondly, the theoretical first-order sea-clutter Doppler frequencies are calculated according to (1) and are mapped to discrete Doppler bin positions. The resulting vector is an all-zero vector, containing only ones at the theoretical positions of the the two Bragg lines, i.e. (3)

$$s_k = \left\{ \begin{array}{ll} 1 & \text{if} \quad k = G(\pm f_d) \\ 0 & \text{else} \end{array} \right\}, \qquad k = 1, \ldots, K \tag{3}$$

where G illustrates the mapping function from continous to discrete. In the third step a cross-correlation of (2) and (3) is calculated by

$$v_k = \sum_{m=\max(1,1-k)}^{\min(K,K-k)} s_m \cdot p_{k+m} \quad (1-K) \leq k \leq (K-1). \tag{4}$$

B. Estimation of the first-order sea-clutter extent in Doppler domain

From (4) in combination with a maximum search it is possible to determine the two actual center first-order sea-clutter Doppler-bin positions named l and m. The correlation is needed to account for a potential Doppler shift of the Bragg-lines due to an underlying sea current [9]. Additional assumptions of the estimation are 1.) first-order sea-clutter is stronger than the second-order sea-clutter and 2.) negative and positive Bragg line experience a Doppler shift into the same direction.

With the help of a local minimum search surrounding the Doppler-bin positions l and m on the summed up range values of (2) it is possible to create a set of Doppler-bins describing the extent of the first-order sea-clutter in Doppler domain as

$$Z = \{l-b_1, \ldots, l, \ldots, l+b_2, m-b_3, \ldots, m, \ldots, m+b_4\}, \tag{5}$$

where b_1, b_2, b_3, b_4 are used to denote the lower and upper limit of the receding and the approaching first-order sea-clutter, respectively. Here it should be noted that due to the finite antenna resolution of any real antenna system the Bragg lines are not, as theory suggests, two discrete frequencies but experience a certain Doppler extent.

C. External noise estimation and estimation of the first-order sea-clutter extent in range domain

In this part an estimation of the external noise level is performed. The estimation avoids the first-order sea-clutter dominated Doppler bins noted in (5) and only utilizes distant range bins to obtain the average external noise power

$$P_{\text{noise}} = \frac{1}{N-w+1} \cdot \frac{1}{K-|Z|} \cdot \sum_{n=w}^{N} \sum_{\substack{k=1 \\ k \notin Z}}^{K} P_{k,n}, \tag{6}$$

in which $|Z|$ denotes the cardinality of the set Z and w is used as starting range bin.

After that the first-order sea-clutter extent in range dimension for the set of Doppler bins Z on the $P_{k,n}$ values is determined. This is performed by static thresholding, derived from the estimated external noise power (6). To avoid assigning targets in noise but close to the clutter edge, the extent of sea-clutter in Doppler domain is only allowed to shrink with range.

Finally the first-order sea-clutter segmentation results and the external noise estimation results are fused into the second-order sea-clutter segmentation process. Knowing the extent and position of the first-order sea-clutter, combined with a local minimum search on the data in (2) and the thresholding approach the second-order sea-clutter segmentation process will be performed in a similar manner as for the first-order. Eventually one final segmentation mask is created.

IV. Adaptive CFAR detection and Pretracker

A. Review CFAR detection

The group of CFAR algorithms are sliding window techniques to detect targets in a clutter/noise background with a predefined probability of false alarm. They estimate the clutter/noise power in the current cell under test (CUT) by inspecting the cells in their local neighborhood, also known as reference cells. Originally designed for a homogeneous background, then extended to multiple-target or clutter-edge scenarios, several variants such as cell-averaging (CA), cell-averaging greatest-of (CAGO), cell-averaging smallest-of (CASO) or ordered-statistic (OS) CFAR have been developed and are commonly used [10] [11].

In all approaches the CUT is compared to a threshold S to make a binary target decision, where S is defined by

$$S = T \cdot Z, \tag{7}$$

in which Z is the local clutter/noise estimation and T denotes the constant scale factor. To maintain a targeted P_{fa} the constant scale factor T has to be determined, where T itself is a function of type of noise/clutter distribution, the type of CFAR and the number of reference cells N_{total}.

In case the detection background consists of independent and identically distributed (i.i.d.) random variables following an exponential distribution and assuming CA-CFAR processing, T can be calculated according to

$$T = N_{\mathrm{total}} \cdot \left(P_{\mathrm{fa}}^{-\frac{1}{N_{\mathrm{total}}}} - 1 \right). \tag{8}$$

Several CFAR approaches to cope with nonhomogeneous background have been proposed. One approach is the already introduced OS-CFAR [4]. Here the reference cells are first rank-ordered and the rth largest value is taken as clutter/noise estimate. With appropriate choice of r this enables to cope with multiple target situations and clutter-edges.

Other approaches also take into account local background information and can be considered combinations of the before mentioned. This includes composite CFAR [3], which changes between CA- and OS-CFAR depending on whether the background is homogeneous or nonhomogeneous and an extension of the composite CFAR idea called adaptive-order statistic (AOS) CFAR [5], which adapts the r parameter of OS-CFAR according to the composition of the background. The variability-index (VI) CFAR [6] is another option, which only selects part of the reference window for the background estimation. Still all these approaches have the shortcomings of only using local information from their predefined reference cells while ignoring global information.

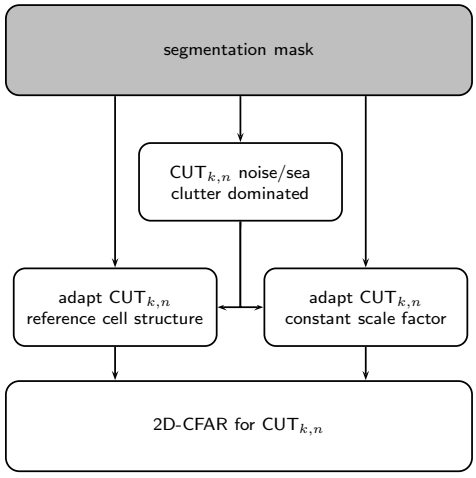

Fig. 2. Adaptive CFAR for particular CUT with reference window shape and constant scale factor adaptation

B. Proposed Adaptive CFAR

The input to adaptive CFAR are the segmentation mask and the range-Doppler map. In addition, parameters like initial shape of the reference window and the type of CFAR noise/clutter estimation have to be provided. Here N_{RI} and N_{DI} are used to denote the number of initially chosen range- and Doppler reference cells. The block structure of our proposed adaptive CFAR is illustrated in Fig. 2. The approach utilizes the segmentation mask to adapt the shape of the reference window and the constant scale factor. As in most CFAR approaches the detection is performed sequentially for each CUT.

The first step is to determine if the current CUT is dominated by external noise or sea-clutter. Based on this outcome the neighborhood of the CUT in the segmentation mask is investigated. If the initial reference window following from N_{RI} and N_{DI} crosses a Doppler-domain clutter-edge the number of reference cells in the Doppler-domain are reduced from N_{DI} to N_{DO}. This happens at the expense that the number of range cells are increased from N_{RI} to N_{RO} to fulfill

$$N_{\mathrm{RI}} + N_{\mathrm{DI}} = N_{\mathrm{RO}} + N_{\mathrm{DO}} = N_{\mathrm{total}}. \tag{9}$$

The underlying idea is that the clutter-edges in the Doppler domain are more abrupt than their counterpart in range-domain and thus the error in the clutter/noise estimation by including non-homogeneous cells in range has less influence. This can

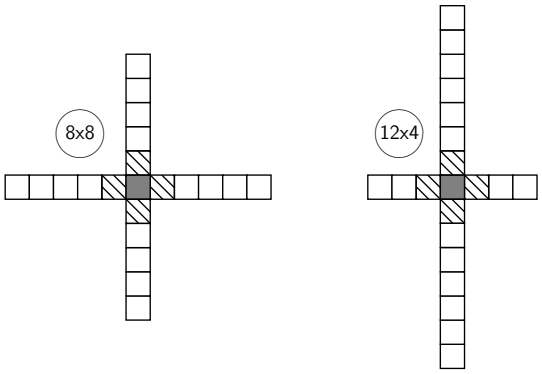

Fig. 3. Example of reference window adaptation

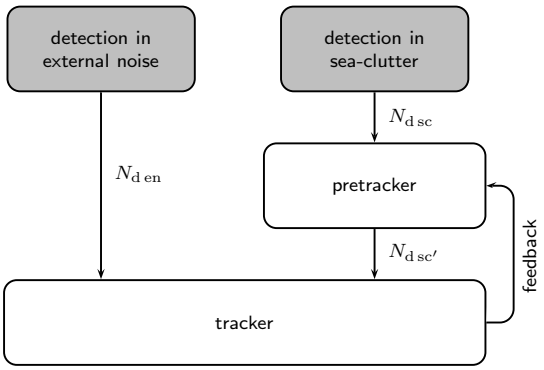

Fig. 4. Pretracking structure

lead to asymmetrically shaped reference windows, still the number of total reference cells N_{total} is maintained. One example of the non-adapted and the adapted reference window with N_{RI} equal to 16 is shown in Fig. 3.

In a parallel step the constant scale factor T for each CUT is adapted. Due to the segmentation it is possible to choose two different T factors independently: one for the external noise dominated regions and one for the sea-clutter dominated regions. As the shape of the reference window has been adapted to obtain a homogeneous detection background, but the total number of reference cells has been maintained, the constant scale factor T is only a function of parameter P_{fa} (8). This allows choosing different T values to allow different P_{fa} in each region. Eventually the 2-dimensional CFAR for each CUT with adapted reference window and adapted scale factor is carried out and a binary target decision is made.

C. Pretracker

If one compares the total number of cells dominated by noise or sea-clutter one clearly realizes that the external noise dominated regions outnumber their counterpart manifold. From this ratio we conclude that we can allow a higher P_{fa} (and thus also higher probability of detection P_{D}) in the clutter dominated part, while choosing a lower P_{fa} in the external noise dominated part.

Without the presegmentation, a single T factor would be used for the complete data set, which would either lead to excessive false alarms or missed targets. If the overall number of false alarms still exceeds the tracking capabilities of the system, a pretracker structure [12] might be used, which differentiates between weak targets and strong targets.

In our case we consider the detections in external noise as strong targets, which are directly forwarded to the tracker, while the detections in the sea-clutter dominated regions are feed to a pretracker structure as illustrated in Fig. 4. Here $N_{\mathrm{d\,en}}$ and $N_{\mathrm{d\,sc}}$ are used to denote the number of detections in external noise or sea-clutter, respectively.

Initially the pretracker forwards all detections in the sea-clutter region to the tracker and thus $N_{\mathrm{d\,sc}}$ is equal to $N_{\mathrm{d\,sc'}}$. In case the number of possible tracks by the sum of $N_{\mathrm{d\,en}}$ and $N_{\mathrm{d\,sc'}}$ is reached, the tracker provides feedback to the

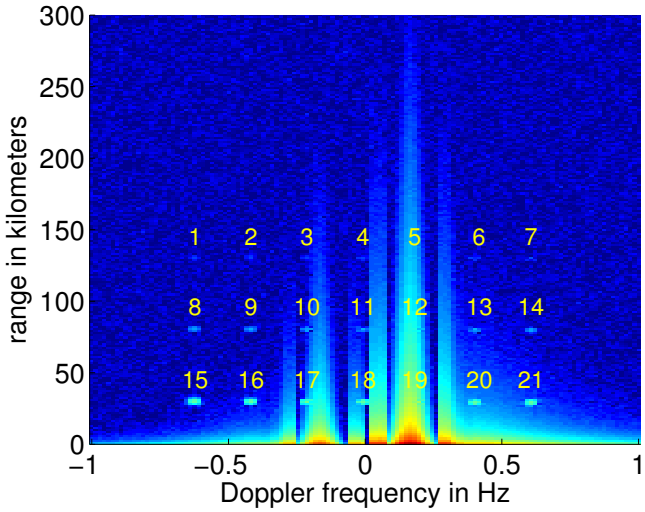

Fig. 5. Range-Doppler Map with labeled targets

pretracker to reduce the number of forwarded detections in sea-clutter $N_{\mathrm{d\,sc'}}$, with $N_{\mathrm{d\,sc'}}$ now being smaller than $N_{\mathrm{d\,sc}}$. This reduction is achieved by only forwarding the $N_{\mathrm{d\,sc'}}$ most reliable detections, which could be identified by additional processing of temporal- or spatial-samples.

V. Evaluation

The evaluation has been performed on simulated data containing 21 targets, embedded in external noise and sea-clutter. The targets have the same Radar Cross Section (RCS) of 20 dBm^2 and are situated at three different ranges of 30, 80 and 130 km and seven different radial speeds corresponding to a Doppler frequency of -0.62 Hz to +0.62 Hz as illustrated in Fig. 5. The first-order sea-clutter lines are situated at $\pm$ 0.2 Hz, each surrounded by second-order sea-clutter. Due to the different radial speed and different ranges of the targets, the targets are situated in different detection background. For the following discussion each target is labeled by a corresponding number from 1 to 21.

The results of the segmentation process according to the descriptions in Section III can be seen in Fig. 6. The segmentation mask is used by the adaptive CFAR to determine the shape of the reference window and the constant scale factor as

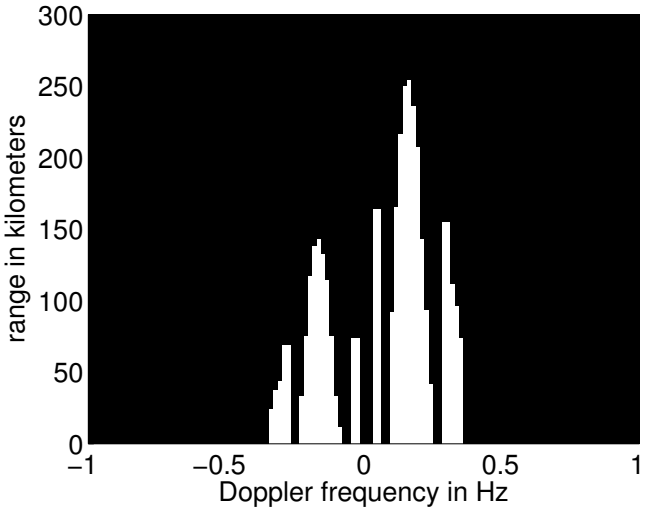

Fig. 6. Combined segmentation mask

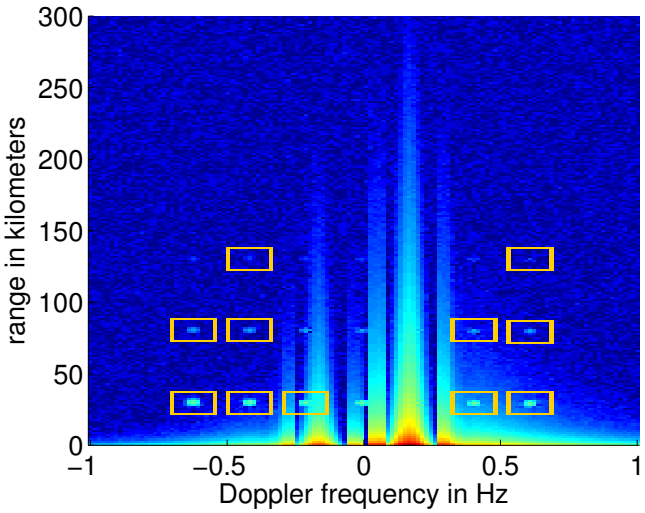

Fig. 7. Detection result of non-adaptive 8x8 CA-CFAR

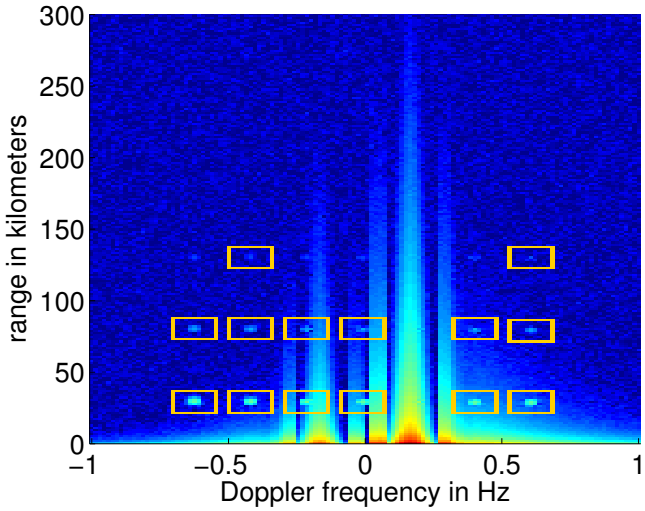

Fig. 8. Detection result of adaptive 8x8 CA-CFAR with reference window shape adaptation

illustrated in Fig. 2. Here it should be mentioned that after all detections an adjacent-detection merging algorithm (ADMA) [13] has been applied. It can be considered a local peak detection to eliminate multiple detections from the same target.

To show the differences in detection performance, four detection examples are illustrated, where in each example the total number of reference cells is chosen to be 16 with a single guard cell surrounding the CUT in each dimension.

First, a non-adaptive 2-dimensional CA-CFAR with N_{RI} as well as N_{DI} chosen to be equal to eight reference cells, is applied. The results of this detection process are shown in Fig. 7. As expected the results show that the target detection in external noise works well (targets 8,9,13,14,15,16,20,21). In case of detecting the most distant targets in external noise (1,2,6,7) only the detection of targets 2 and 7 are successful, which can be explained by a lack of reflected signal power. If the targets are situated close to a Doppler clutter-edge (targets 3,4,10,11,17,18) only the detection of target 17 is successful. The detection of any of the targets in the approaching first-order sea-clutter (targets 5,12,19) is not possible.

Second, the proposed adaptive 2-dimensional CA-CFAR with same initial reference cell configuration as in the first case is applied. In this case the reference window shape might be adapted but the total number of reference cells N_{total} is maintained. In this case the detection results are shown in Fig. 8. The number of detections in external noise remain the same as for the non-adaptive case, which is due to the fact that the shape of the reference window is kept unchanged. The detection results at the clutter edges is improved from a single detection (target 17) in the non-adaptive case to four successful detections (targets 10,11,17,18) by the adaptation of the reference window.

Third, the adaptive CFAR with reference window shape adaptation and constant scale factor adaptation is applied, with detection results illustrated in Fig. 9. This case is chosen to illustrate how it is possible to allow a higher P_{fa} (lower constant scale factor) in the sea-clutter dominated part, but maintain the same P_{fa} (as before) in the noise dominated part.

Allowing a higher P_{fa} implicitly also increases the P_{D}, which explains that the adaptive CFAR now indicates additional detections in the sea-clutter dominated parts. In two cases the detection can be attributed to the presence of a target (target 12,19) in the first-order sea-clutter, in all other cases a false-alarm occurs. In case an even higher P_{fa} in the sea-clutter dominated part is allowed and the tracker is driven into saturation, the application of a pretracker is justified.

The fourth case, shown in Fig. 10, is again a non-adaptive CFAR detection with a global lower constant scale factor and a resulting increase in P_{fa}. This case illustrates how this could lead to a saturation of the tracker. Still it should be noted that in contrast to the previous adaptive case here targets 12 and 19 are not being detected.

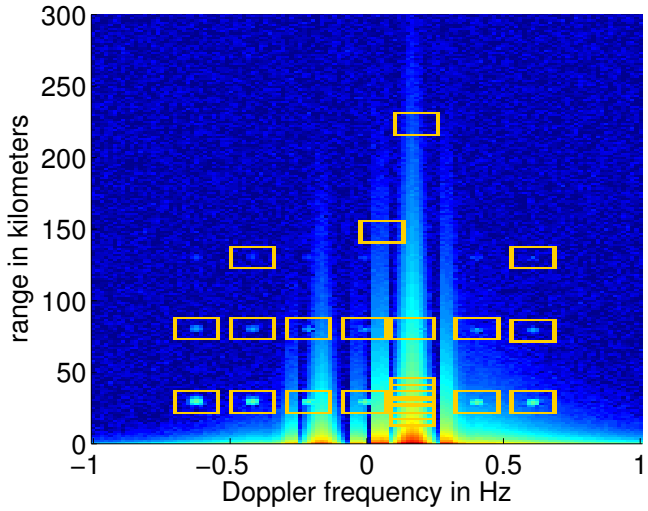

Fig. 9. Detection result of adaptive 8x8 CA-CFAR with reference window shape and constant scale factor adaptation

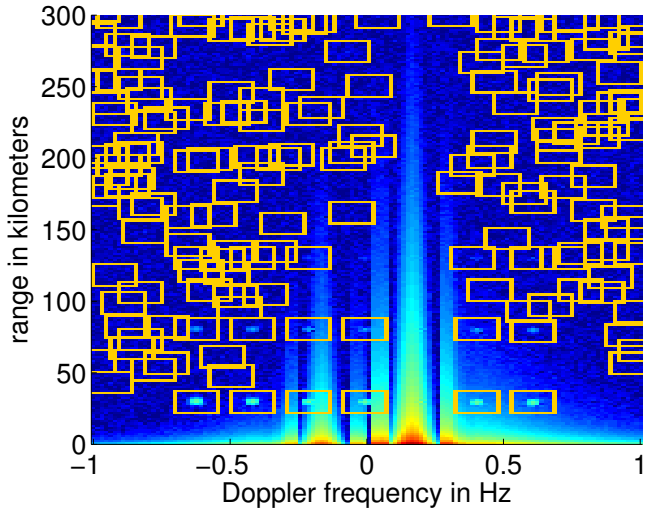

Fig. 10. Detection result of non-adaptive 8x8 CA-CFAR with global higher P_{fa}

VI. Conclusion

In this paper we have presented an adaptive CFAR detection algorithm with global presegmentation and following pretracker structure for HFSWR. In contrast to other (local) CFAR approaches this approach first performs a global adaptation of the reference window shape due to information from presegmentation to obtain homogeneous reference cells. Local CFAR approaches, on the other hand, work on a fixed reference window shape and try to obtain homogeneous reference cells by censoring or an appropriate selection of r parameter in an ordered-statistic approach. This is particularly difficult to be performed for a small number of reference cells.

Furthermore, the presegmentation makes it possible to apply a background dependent threshold selection and allow a higher probability of detection (and higher probability of false alarm) in the sea-clutter dominated areas while keeping a lower probability of false alarm in the external noise dominated areas. The following pretracker structure prevents the saturation of the tracker by weak detections.

Acknowledgment

This work was supported by Wehrtechnische Dienststelle für Schiffe und Marinewaffen, Maritime Technologie und Forschung (WTD 71), Eckernförde, Germany.

References

[1] M. Turley, "Hybrid CFAR techniques for HF radar," in *Radar 97 (Conf. Publ. No. 449)*, Oct. 1997, pp. 36 –40.

[2] D. Barrick, "Remote sensing of sea state by radar," in *IEEE International Conference on Engineering in the Ocean Environment (Ocean) 72* , Sept. 1972, pp. 186 –192.

[3] R. Nitzberg, "Composite CFAR techniques," in *Conference Record of The Twenty-Seventh Asilomar Conference on Signals, Systems and Computers*, Nov. 1993, pp. 1133 –1137 vol.2.

[4] H. Rohling, "Radar CFAR Thresholding in Clutter and Multiple Target Situations," *IEEE Transactions on Aerospace and Electronic Systems*, vol. AES-19, no. 4, pp. 608 –621, July 1983.

[5] P. Gandhi and S. Kassam, "An adaptive order statistic constant false alarm rate detector," in *IEEE International Conference on Systems Engineering, 1989*, Aug. 1989, pp. 85 –88.

[6] M. Smith and P. Varshney, "Intelligent CFAR processor based on data variability," *IEEE Transactions on Aerospace and Electronic Systems*, vol. 36, no. 3, pp. 837 –847, July 2000.

[7] D. Barrick, "First-order theory and analysis of MF/HF/VHF scatter from the sea," *IEEE Transactions on Antennas and Propagation*, vol. 20, no. 1, pp. 2 – 10, Jan. 1972.

[8] M. Xiangwei, G. Jian, and H. You, "CFAR techniques for over-the-horizon radar," in *IEEE International Symposium on Intelligent Signal Processing 2003*, 2003, pp. 83 – 85.

[9] K.-W. Gurgel, "Remote Sensing of Surface Currents and Waves by the HF Radar WERA," in *Seventh IEE Conference on Electronic Engineering in Oceanography*, June 1997, pp. 211 –217.

[10] P. Gandhi and S. Kassam, "Analysis of CFAR processors in homogeneous background," *IEEE Transactions on Aerospace and Electronic Systems*, vol. 24, no. 4, pp. 427 –445, July 1988.

[11] A. Dzvonkovskaya and H. Rohling, "CFAR Target Detection Based on Gumbel Distribution for HF Radar," in *International Radar Symposium (IRS) 2006*, May 2006, pp. 1 –4.

[12] E. J. Hughes and M. Lewis, "Adaptive Spatio-Temporal CFAR and Multiple-Hypothesis Tracking System," *Staff publications - Cranfield Defence and Security*, 2009, last accessed 29-02-2012. [Online]. Available: http://dspace.lib.cranfield.ac.uk/handle/1826/3264

[13] G. Trunk, "Range Resolution of Targets Using Automatic Detectors," *IEEE Transactions on Aerospace and Electronic Systems*, vol. AES-14, no. 5, pp. 750 –755, Sept. 1978.